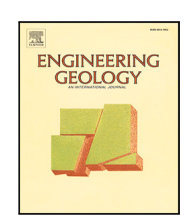
\$ 50 CONTRACTOR OF THE SECOND SECOND

Contents lists available at ScienceDirect

Engineering Geology

journal homepage: www.elsevier.com/locate/enggeo





Numerical study on the stiffening properties of scour protection around monopiles for Offshore Wind Turbines

Carlos Menéndez-Vicente ^a, Susana López-Querol ^a, John M. Harris ^b, Nicholas S. Tavouktsoglou ^b

- a University College London, Gower Street, London, WC1E 6BT, United Kingdom
- ^b HR Wallingford, Howbery Park, Wallingford, OX10 8BA, United Kingdom

ARTICLE INFO

Keywords: Scour Scour protection Monopiles Offshore wind turbines Soil structure interaction Geohazard

ABSTRACT

An active marine seabed causing scour around monopile foundations has to be addressed as a geological hazard. These structures are often protected with rock armour to prevent foundation failure. However, scour protection also increases the confining pressure and embedment length, providing additional stiffness to the soil-pile system. This study focuses on the stiffening effect of scour protection to optimise foundation design. A parametric analysis of the dimensions and materials of scour protection is carried out with more than 100 simulations to assess the stiffening effect of scour protection. Therefore, small-diameter and large-diameter monopiles are investigated. Numerical analysis with the Finite Element method is conducted to estimate the natural frequencies and the static capacity through moment and lateral load (M-H) curves and the Load Utilisation method. These methods, which are new to the study of scour protection, are proposed for the quantification and assessment of scour protection in foundation design. The results show that rock fill restores the initial foundation conditions independently of the pile dimensions. While for small-diameter monopiles, scour protection fulfils its double purpose of preventing scour and providing stiffness to the foundation, for large-diameter monopiles the contribution to the stiffness is limited and should only be considered for heavy rock armour and significant scour protection heights. The parametric analysis indicates that a thicker and heavier scour protection increases the static capacity by 10%, whereas the width or a densification through sand accretion have negligible effects (<1%). The M-H curves and the Load Utilisation method have shown to be effective in assessing the static capacity of monopiles supporting Offshore Wind Turbines.

1. Introduction and background

The marine geology affects the foundation capacity and lifetime performance of Offshore Wind Turbines (OWTs). Geological marine phenomena and hazards such as bedform migration, slope failures, scour around monopiles, or seismic-induced liquefaction threaten the stability and operability of OWTs (Zhu et al., 2023).

Large soil volume movements can occur within a short time interval as reported in Harris et al. (2019), where a scour hole slope failure comprised the movement of 430 m³ of sand in a time interval of 75 min. Further submarine geological processes, such as landslides, are likely to change the seabed morphology. Weakly sloped sediments subjected to large stresses caused by storm events, earthquakes, and high internal pore pressures can lead to thousands of cubic kilometres of material volume to be moved over large distances (Hampton et al., 1996). An example of this is the Storegga slide in the Norwegian Sea that comprised the movement of approximately 3600 km³ of material

over 1600 km (Harris et al., 2019). All these phenomena may take place without even noticing them. Monitoring vast ocean areas is nowadays a difficult but important task with the increasing need to expand the boundaries of offshore wind power.

An example of failure due to scour is found in the Robin Rigg Offshore Wind Farm (OWF), where massive scour depths were observed, altering the eigenfrequency, and compromising the turbine's operability (G+ Offshore Wind, 2017). Scouring and large-scale movement of the sandbank system at the Robin Rigg OWF finally led to the decommissioning of two turbines.

The geological characterisation of the soil on vast ocean areas is often linked with a high variability (Le et al., 2014) and parametric uncertainty (Hsu et al., 2022). Soils from sands to clays respond differently to monotonic and cyclic loading, inducing changes in their stiffness (e.g. degradation), shearing response, and material failure (e.g. Zhou et al., 2017; Pan et al., 2022). Scour is normally addressed as

E-mail address: carlos.vicente.19@ucl.ac.uk (C. Menéndez-Vicente).

^{*} Corresponding author.

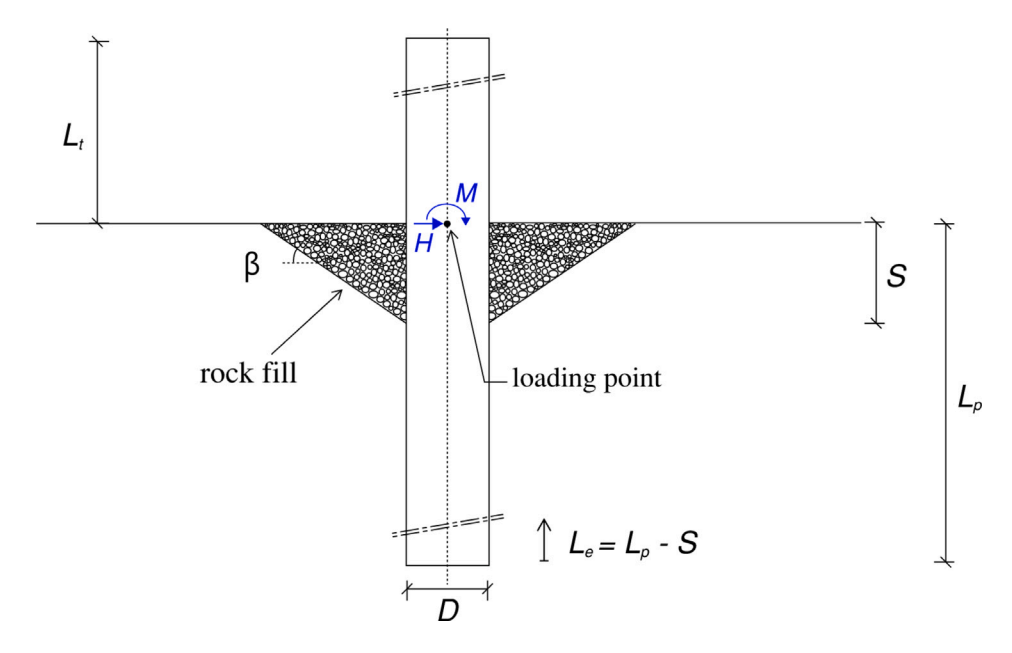


Fig. 1. Scoured monopile with rock fill as scour protection system.

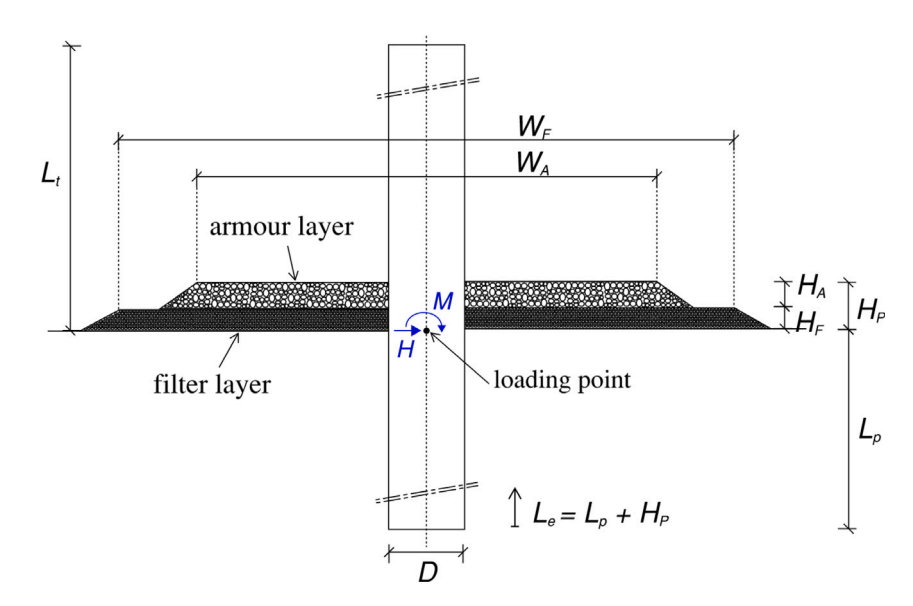


Fig. 2. Monopile with pre-installed rock as scour protection system.

a hydrodynamic problem by engineers focusing on fluids. However, to the authors' opinion, scour also requires a geological and geotechnical approach. Our study intends to raise awareness within the engineering geology community about the real hazard that scour poses to OWTs. To enhance the safety of these foundations, scour protection systems that provide stability and reduce geological uncertainties should be put forward and deeply investigated.

Different protection methods have been installed in marine and fluvial environments (non-exhaustive list): rock armour (also known as riprap), filled bags or nets, concrete or geotextile mattresses (Tavouktsoglou, 2018; Mayall et al., 2020), or collar protections. Rock scour protection is often constructed with an armour layer and one or more granular underlayers or filter layers. Typically scour protection is placed as a single layer system, where the filter and armour are incorporated within a single rock layer comprised of a widely graded rock, or as a two–layer system comprised of a separate filter and armour. The purpose of a filter layer in a scour protection system is to minimise the loss of finer sediment derived from the seabed whilst remaining permeable enough for the water to flow through it. The

armour layer provides the necessary resistance to the hydrodynamic loads. Such a protection system consisting of loose rock has been installed in many OWFs due to its ease of deployment and adaptability to changes in seabed level and edge scour. Tables 1 and 2 show examples of European wind farms founded with monopiles in sands and protected against scour. The geometric parameters in these tables describe the foundation and the scour protection dimensions and are explained in Figs. 1 and 2. The diameter of the pile is D, the pile length is L_p , the widths of the filter and armour layers are W_F and W_A , and the heights of the filter and armour layers are \mathcal{H}_F and \mathcal{H}_A . The parameters d_{50} and D_{n50} refer to the median (nominal) diameter of the soil and rock respectively, and M_{50} refers to the median mass of the rock. Focusing on the dimensions, Table 2 shows that scour protection designs cover an overall height ranging from 1.5 m to 2.8 m, and an overall width of 4 to 6D, with D as the diameter of the monopile. These systems have proven to be effective in preventing scour (Matutano et al., 2014) and are the State-of-the-Art of foundation design and scour protection strategies.

Table 1
Post-installed scour protections (rock fill) in existing OWF founded on monopiles in sands (data from Whitehouse et al. (2011)^(a) and Esteban et al. (2019)^(c)).

Wind farm	ind farm Foundation			Rock fill
	<i>D</i> [m]	L_p [m]	d ₅₀ [mm]	
Arklow Bank Scroby Sands	$5.0^{(a,c)}$ $4.2^{(a,c)}$	35 ^(c) 30 ^(c)	$0.20^{(c)} \ 0.40^{(c)}$	$D_{n50} = 0.42 \text{ m } (M_{50} = 200 \text{ kg})^{(a)}$ $D_{n50} = 0.15 \text{ m } (0.01 \text{ m} < d < 0.3 \text{ m})^{(a)}$

Table 2
Pre-installed scour protections (riprap) in existing OWF founded on monopiles in sands (data from Whitehouse et al. (2011)^(a), Matutano et al. (2014)^(b), and Esteban et al. (2019)^(c)).

Wind farm	Foundation			Filter lay	Filter layer			Armour layer		
	<i>D</i> [m]	L_p [m]	d ₅₀ [mm]	W_F [m]	H _F [m]	D _{n50,F} [m]	W _A [m]	<i>H_A</i> [m]	D _{n50,A} [m]	
Arklow Bank	5.0 ^(a,c)	35 ^(c)	0.20(c)	20 ^(c)	0.6(c)	0.05 ^(c)	15 ^(c)	1.2(c)	$0.42^{(b,c)}$	
Egmond aan Zee	$4.6^{(b,c)}$	30 ^(c)	$0.20^{(c)} \ 0.25^{(a)}$	$24^{(a,c)}$	0.4(c)	$0.05^{(a,c)}$	$18^{(b,c)}$	$1.4^{(b)}$ $1.8^{(c)}$	$0.40^{(a,c)}$	
Horns Rev	$4.2^{(b,c)}$	34 ^(c)	$0.15^{(c)} \ 0.50^{(a)}$	$20^{(a,c)}$	$0.5^{(b)} \ 1.0^{(c)}$	$0.1^{(a)} \ 0.2^{(b)}$	15 ^(c)	$1.0^{(b)}$ $1.8^{(c)}$	$0.4^{(a,b)}$ $0.55^{(c)}$	
Princess Amalia Scroby Sands	$4.0^{(c)}$ $4.2^{(a,c)}$	$30^{(c)}$	0.578 $0.40^{(c)}$	$24^{(c)}$ $25^{(c)}$	$0.9^{(c)} \ 1.0^{(c)}$	$0.17^{(c)} \ 0.15^{(b,c)}$	$18^{(c)}$ $15^{(c)}$	$1.5^{(c)}$ $1.3^{(c)}$	$0.50^{(c)} \ 0.45^{(c)}$	

Researchers frequently apply an experimental approach in their scour protection studies, which mainly focus on the design of the scour protection system (De Vos et al., 2011 and 2012), its performance (Whitehouse et al., 2011), its integrity (Whitehouse et al., 2014; Xu et al., 2022) or the integrity of the surroundings of the scour protection system (Sarmiento et al., 2021), rather than analysing the contribution of scour protection to the foundation stiffness. However, a few experimental studies analyse the effects of scour protection from the geomechanical and structural point of view. Mayall et al. (2020), for instance, studied the impact on the natural frequencies of two postscour (or remedial) protection systems (tire-filled nets and rock fill), and one pre-scour protection system (rock armour) for a monopiletower system in the Fast Flow Facility (FFF) flume at HR Wallingford (UK). This is one of the few studies that analyses the structural impact of scour protection systems in terms of (i) scour protection performance and (ii) changes in the foundation stiffness. They concluded that preinstalled systems contributed significantly to the dynamic performance of the foundation, whereas remedial scour protection systems failed to restore the foundation stiffness prior to scour. Moreover, they observed that sand accretion in the scour protection may also provide foundation stiffening (also in Mayall, 2019). However, to the authors' knowledge, the influence of a time-dependent densification of the riprap matrix due to sand accretion (or even marine growth depending on the water depth) has not been considered yet in terms of their potential increase in foundation stiffness. Thus, more research and close monitoring of existing scour protection matrices is needed.

Numerically, scour protection studies focus on the modelling of the lifting of rock material pieces using Computational Fluid Dynamics (CFD) as published for instance in Nielsen et al. (2013). Moreover, they focus on the hydrodynamic phenomena involved in the loss of individual rock pieces or the sinking of material into the ground, in order to develop design criteria for rock sizes. However, these models are very time-consuming and require significant computational power.

As seen in the literature and concluded in Fazeres-Ferradosa et al. (2021), very few publications adopt numerical approaches to study scour protection from the geomechanical and structural perspective. Mayall (2019) presented a 1D Finite Element (FE) model for the analysis of natural frequencies with scour and scour protection in addition to the physical modelling commented previously. However, this approach simplifies the soil's constitutive law and neglects important 3D effects such as the riprap-pile interface. Chortis (2018) and Saathoff et al. (2024) analysed monopiles with scour and with scour protection with 3D FE modelling in Plaxis using hypoplasticity and Hardening Soil Small Strain (HSS) as constitutive models respectively. The scour

protection layer in Chortis (2018) was simulated using an equivalent surcharge of 15 kPa. From this study, it is concluded that the overburden pressure contributes to the lateral stiffness only in the top soil layers (the contribution to the lower layers is negligible). Askarinejad et al. (2022) used a similar 3D FE model to simulate cyclic loading. Although these studies implemented a complex hypoplastic constitutive model with the simulation of cycle-induced strain accumulation, they approach the modelling of scour protection with a surcharge around the pile, which does not reflect the change in the embedment length and the riprap-pile interface. Numerical modelling to study the effects of scour protection on the eigenfrequency and the lateral response of monopiles was also carried out by Ma and Chen (2021). They suggested that the rock density and the layer thickness of the scour protection system were the main contributors to the stiffness increase in terms of natural frequency and lateral capacity.

These studies provide a solid contribution to the understanding of the positive impact of scour protection on the foundation. Nonetheless, they do not differentiate between the filter and armour layers in terms of material properties and dimensions. Moreover, they do not consider other forms of scour protection systems such as rock fill for a developed scour hole. Finally, no study analyses the load capacity increase due to scour protection in the M-H space in terms of load utilisation for realistic environmental wind and wave loads. The Load Utilisation (LU) method proposed in Aleem et al. (2022) and applied in Menéndez-Vicente et al. (2023) is implemented. This method has proven to be efficient in determining the changes in static capacity for different foundation conditions.

As seen in the literature, studies focus on the design and hydrodynamic performance of scour protection systems exposed to the marine environment. However, these systems, based on adding rock material to the surroundings of the pile, indirectly change the foundation conditions by increasing the soil's confining pressure and the embedment length. In current practice, the industry demands physical models to assess the performance of scour protection systems (Fazeres-Ferradosa et al., 2021). However, designers should also focus on the (possible) beneficial side-effects of scour protection systems to optimise foundation design. This paper aims thus to clarify whether including scour protection systems as a component of offshore piled foundations during design has a beneficial contribution or not. Therefore, in this study the stiffening properties of scour protection are assessed in terms of (i) additional static capacity (moment M and horizontal load H), and (ii) variations in eigenfrequencies for monopiles in sands protected against scour for small-diameter and large-diameter monopiles.

To broaden knowledge in this insufficiently studied field, the Load Utilisation (LU) method is applied and M-H curves are developed in the framework of a parametric study that analyses different scour protection geometries, scour protection systems, and material properties. In the literature, no study applying these methods (LU and M-H curves) to the analysis of scour protection systems can be found. The results presented cover a wide range of parameters and include more than 100 simulations with M-H loading, from which new design recommendations are derived for engineers involved in the foundation design process of piled foundations used in OWT.

2. Methodology

2.1. General approach

M - H curves were constructed and LU ratios were calculated using Finite Element (FE) analysis. The numerical model is based on previous studies from Aleem et al. (2022), Askarinejad et al. (2022), and Menéndez-Vicente et al. (2023). This study uses the LU method to assess the impact of scour protection and to quantify the potential stiffness increase achieved through scour protection. A parametric study is developed to determine which parameters (i.e. scour protection dimensions, material properties, and pile dimensions) influence the foundation stiffness response. As explained in Menéndez-Vicente et al. (2023), the M-H curves are based on simulating failure under monotonic *M* and *H* loads. The failure definition used in LeBlanc et al. (2010) and based on a rotation of 4° was applied. This methodology is efficient in terms of computational time and allows the simulation of many load and parameter combinations to study the stiffness contribution of scour protection and its implications in the static capacity of monopiles subjected to offshore environmental loads. Additionally, natural frequencies were calculated using FE analysis to assess the impact of scour protection on the dynamic performance of OWT protected against scour.

2.2. Numerical model

The FE model built in Ansys static structural (version 2023 R2) consists of one symmetric half of a pile with a length L_p and a diameter D embedded in a soil domain with a length of 22.8D and a height of 8.1D (Askarinejad et al., 2022). In this section, the modelling strategies for the soil, the scour protection systems, and the pile are presented. A large-diameter (D=7.5 m) and a small-diameter (D=1.8 m) monopile were analysed as explained in the next sections.

Soil modelling.

The study analyses the sand response to monotonic lateral force and moment loading. An elasto-plastic Mohr–Coulomb (MC) model was implemented in this paper, as it has been demonstrated to be sufficient to simulate the static nature of the applied monotonic loading. Geba sand (Azúa-González et al., 2019) was chosen for similarity with the centrifuge tests performed by Askarinejad et al. (2022), which were used for model validation. In Table 3, ϕ is the friction angle, c is the cohesion (chosen as 1 kN/m² to avoid convergence issues), ρ_d is the dry density, ν is the Poisson's ratio and E_s is the Young's Modulus. Dry densities were used in the parametric study for simplicity and comparability (validation) with other studies. Nonetheless, the general qualitative conclusions also apply to the submerged environment of OWF. However, this paper also presents representative M-H curves constructed under submerged conditions, which serve as design charts for engineers (Section 3.2).

Table 3
Soil material parameters for the FE model.

Material	φ [°]	c [kN/m²]	ρ_d [t/m ³]	ν [–]	E_s [MN/m ²]
Geba sand	34	1.0	2.0	0.25	32

Scour protection modelling.

Two systems were analysed to cover both scour protection strategies that are usually applied in the field: (i) a post-installed (remedial) scour protection system consisting of filling with rock an already developed scour hole (Fig. 1), and (ii) a pre-installed system, which is formed by a filter layer and an armour layer (Fig. 2). Rock material is classified by its particle size (or weight) distribution. Rock fill or filter layers use coarse grading (CP) materials (e.g. CP 45-125, i.e. sieve size of 45 to 125 mm). Armour layers are typically composed of light grading (LM) products (e.g. LMA 5-40, i.e. light armourstone with a piece weight of 5 to 40 kg). In the current offshore practice, a typical rock fill material used in post-installed solutions is CP 45-180, which presents a wide grading that enables an appropriate fill of the scour hole. For preinstalled solutions, filter layers typically consist of a CP 45-125 and armour layers of LMA 5-40. This latter layer, however, may also be designed with up to LMA 40-200, if larger rock weights are required. Table 4 lists the different scour protection materials used in this study.

The numerical modelling of the scour protection system via FE requires the idealisation of scour protection as a solid body (instead of grain to grain modelling). By analogy to the soil domain, a Mohr-Coulomb (MC) constitutive law was used given the granular nature of the material and the type of loading (i.e. monotonic) as also found in Ma and Chen (2021). A friction angle of $\phi = 45^{\circ}$ was assumed for the riprap material after Hough (1957). Regarding the Young's Modulus, the riprap material presents a higher stiffness compared to the surrounding soil domain. Therefore, a Young's Modulus $E_s = 80 \text{ MN/m}^2$ was chosen to simulate the elastic response of bulk-placed materials. However, for the cases in which densification through sand accretion was studied (i.e. LMA 5-40 densified and very densified), a representative increase of the Young's Modulus of 10 MN/m2 was considered. Depending on the riprap material, the bulk properties vary. Table 4 shows the parameters of the different scour protection materials. The median armourstone piece mass M_{50} (Eq. (1)), the median sieve size D_{50} (Eq. (2)), the single-size void ratio e_0 (for a typical mechanically crushed material), the uniformity coefficient n_{RRD} , the void ratio e (Eq. (3)), the porosity of the bulk-placed material n_{ij} (Eq. (4)), the apparent density of the armourstone ($\rho_{app}=2.65~{\rm t/m^3}$) and the dry bulk density ρ_d (Eq. (5)) were defined after the Rock Manual (CIRIA/CUR/CETMEF, 2007). Densification through sand accretion was considered by decreasing the porosity of the armour layer matrix of the LMA 5-40 to $n_v = 0.4$ (densified: "d+") and $n_v = 0.3$ (very densified: "d++").

$$M_{50} = 0.5(M_{50,min} + M_{50,max}) (1)$$

$$D_{50} = \frac{1}{0.84} \left(\frac{M_{50}}{\rho_{app}}\right)^{1/3} \tag{2}$$

$$e = \frac{e_0}{90} \arctan(0.645 n_{RRD}) \tag{3}$$

$$n_v = \frac{e}{1+e} \tag{4}$$

$$\rho_d = (1 - n_v)\rho_{app} \tag{5}$$

Table 4Scour protection material parameters for the FE model.

	*								
Type	Material	M_{50} $minmax$	D_{50}	e_0	n_{RRD}	e	n_v	ρ_d	E_s
		[kg]	[mm]	[-]	[-]	[-]	[-]	$\left[\frac{t}{\mathrm{m}^3}\right]$	$\left[\frac{MN}{m^2}\right]$
Rock fill	CP 45-180	-	98	0.94	2.41	0.598	0.374	1.66	80
Filter	CP 45-125	-	80	0.94	3.28	0.676	0.403	1.58	80
Armour	LMA 5-40	14-28	234	0.94	5.22	0.767	0.434	1.50	80
	LMA 40-200	101-152	424	0.94	6.74	0.805	0.446	1.47	80
	LMA 5-40 (d+)	14-28	237	_	_	0.667	0.400	1.59	90
	LMA 5-40 (d++)	14-28	237	-	-	0.429	0.300	1.86	100

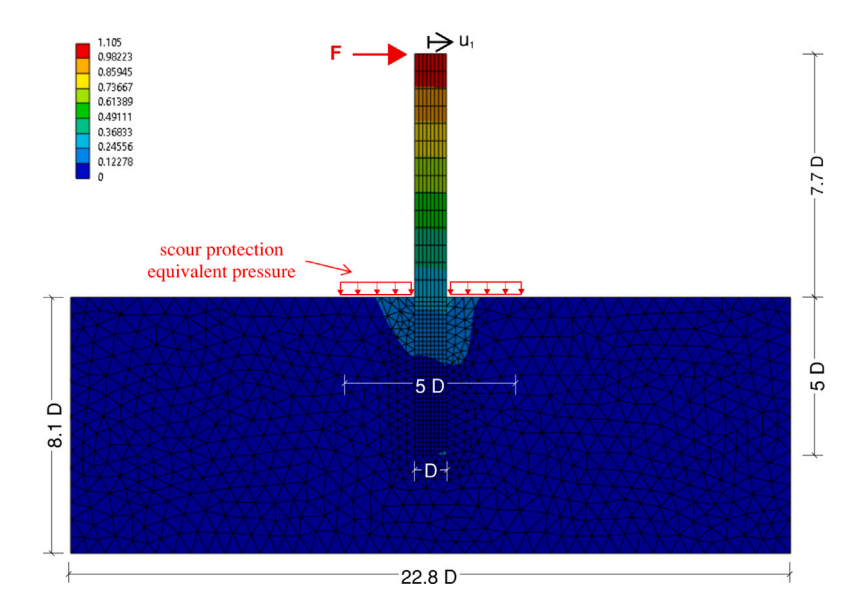


Fig. 3. Horizontal displacements in [m] obtained for validation of the model by Askarinejad et al. (2022).

Structure modelling.

The monopile was modelled with isotropic linearly elastic structural steel. Therefore, the tubular structure was replaced by a solid body with equivalent flexural stiffness and masses after Lopez-Querol et al. (2020). Two different monopiles were analysed. Firstly, in line with the example from Askarinejad et al. (2022) used for validation, a small-diameter monopile with D = 1.8 m was studied. Moreover, a large-diameter monopile with D = 7.5 m, as used in previous studies (Menéndez-Vicente et al., 2023), was also considered. The chosen diameters are representative cases for small-diameter and largediameter piles. Tables 5 and 6 show the material parameters of both soil-pile systems used for the FE model, where W is the weight of the body (including the weight of the sand inside the pile) and I is the moment of inertia. To allow comparability between the small and the large-diameter monopiles, the geometric parameters $(D, t, L_n, L_t, and$ the domain dimensions) of the small-diameter model in Askarinejad et al. (2022) were scaled up via the pile diameter D. Hence, the embedment length to pile diameter ratio $L_p/D = 5$, the tower length to pile diameter ratio $L_t/D = 7.7$, and the diameter to the tubular steel wall thickness ratio D/t = 58 (i.e. the bending stiffness EI) were kept identical in both systems. The structure behaves rigidly, leading to failure caused by a solid body rotation rather than by internal bending.

The interface between the structure and the surrounding soil or riprap material was simulated for the small-diameter monopile with a rough condition following Askarinejad et al. (2022) and assuming full soil plug conditions. This rough soil–pile interface was validated as seen in Section 2.5. This assumption may be applicable for the studied (small-diameter) dimensions. However, other examples in the literature that consider large-diameter monopiles use a friction law with a coefficient of 0.4 (Achmus et al., 2009) for the soil–pile interface. For large-diameter monopiles, a certain amount of sliding (or even

slight separation) between the surrounding soil and the pile may be expected as concluded in e.g. Cuéllar (2011). Therefore, these two different diameter-dependent definitions of the soil–pile interface were applied for consistency with the literature. To verify whether these different interface definitions have a significant influence on the M-H curves, the validation example in Fig. 4 (small-diameter pile) was also analysed with a friction law. The results show that the rough condition is more appropriate to simulate the soil–pile interface for small-diameter monopiles.

Limitations.

The numerical model described previously may be used for the simulation of monotonic loading applied to the soil-pile system. As is intended in the present study, different parameters affecting the M-Hcapacity and natural frequencies are analysed. In an active marine geological environment, loads such as wind and wave are cyclic. This type of cyclic loading may induce changes in the soil stiffness and the granular matrix, for which the aforementioned MC model is not appropriate. Bearing in mind this limitation, the current modelling technique is useful for the estimation of static capacities and natural frequencies. For the analysis of cyclic loads on monopiles supporting OWT, the implementation of a constitutive model that accounts for the simulation of the ratcheting phenomenon (i.e. accumulation of displacements after each load cycle) is needed, which is a future prospect of the present study. Moreover, the analysis of cyclic loading on the soil response may shed light into the effects of scour or scour protection on changes in the granular matrix and potential densification effects. These type of loading and analyses are out of the scope of the present study.

Table 5
Structure material parameters of the small-diameter monopile for the FE model.

Structure	Туре	<i>D</i> [m]	<i>t</i> [m]	<i>L</i> [m]	W [t]	$ ho_d$ [t/m ³]	ν [–]	E_s [GN/m ²]	<i>I</i> [m ⁴]
Pile	tubular	1.8	0.031	9.00	27.45	7.86	0.3	210	0.067
Pile	solid	1.8	-	9.00	27.45	2.40	0.3	27.51	0.515
Tower	tubular	1.8	0.031	13.86	9.38	7.86	0.3	210	0.067
Tower	solid	1.8	-	13.86	9.38	0.532	0.3	27.47	0.515

Table 6Structure material parameters of the large-diameter monopile for the FE model

Structure	Type	<i>D</i> [m]	t [m]	<i>L</i> [m]	W [t]	$ ho_d$ [t/m ³]	ν [–]	E_s [GN/m ²]	<i>I</i> [m ⁴]
Pile	tubular	7.5	0.129	37.5	1985	7.86	0.3	210	20.29
Pile	solid	7.5	-	37.5	1985	2.40	0.3	27.47	155.32
Tower	tubular	7.5	0.129	57.75	678	7.86	0.3	210	20.29
Tower	solid	7.5	-	57.75	678	0.531	0.3	27.44	155.32

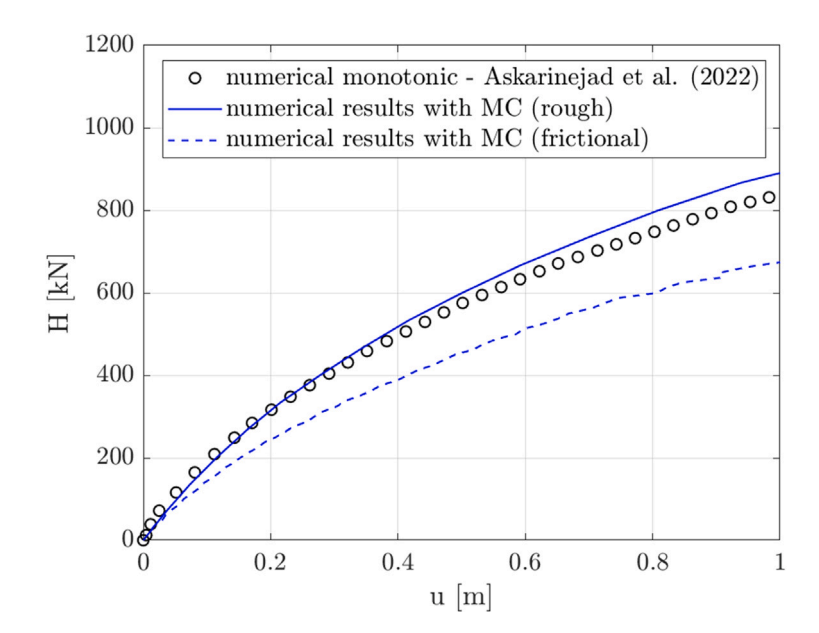


Fig. 4. Validation of the monotonic test performed in Askarinejad et al. (2022) through numerical modelling with MC in Ansys of a monopile with a scour protection equivalent pressure.

2.3. Parametric study

This study focuses on the parameters (i.e. dimensions and material properties) of different scour protection systems and analyses their contribution to the foundation stiffness in terms of M-H capacity improvement and impact on the natural frequencies. Failure is simulated through FE analysis with horizontal loads H and moments Mthat were applied to the monopile at mudline level (Figs. 1 and 2). This loading point was chosen to apply the horizontal force and the moment loading separately. A horizontal load applied at the top of the structure, i.e. the loading point in Askarinejad et al. (2022), which was used for validation, would have induced not only lateral forces but also moment loading $(M_{mudline} = H_{top} * h$, with $M_{mudline}$ as the moment at mudline level, H_{ton} as the horizontal load at the top of the structure, and *h* as the structure's height). Hence, the loading point was chosen for convenience for all models at mudline level. This approach is consistent with other publications (e.g. Aleem et al., 2022) and with previous work (Menéndez-Vicente et al., 2023). It is noted that this loading point is only used for the construction of the M-H curves. For real OWT analysis with the modelisation of the structure under real wind-wave loading, each load must be applied at the corresponding level.

Typical modes of failure of scour protection systems that involve damage in the riprap layers (e.g. erosion, loss of sediment grains through the scour protection layers), secondary scour (i.e. edge scour) or the sinking of rock pieces into the ground (Whitehouse et al., 2011), are local hydrodynamic phenomena and thus out of the scope of the present study.

Table 7 lists the studied parameters. Firstly, remedial rock fill (Fig. 1) of scour holes with a scour depth of 0.5D and 1.0D was analysed. In Fig. 1, β is the angle of the scour hole. Secondly, preinstalled scour protection systems (Fig. 2) were studied considering the following parameters: width and height of the riprap bodies, material of the rock armour layer, and densification of the rock armour layer through sand accretion. The parametric study was designed based on examples of existing wind farms found in the literature (Hansen et al., 2007, Louwersheimer et al., 2009, Raaijkmakers, 2009, Whitehouse et al., 2011, Matutano et al., 2014, and Esteban et al., 2019) and from the authors' experience at HR Wallingford.

The chosen range of rock armour width was 3.5D to 4.5D. A minimum rock armour width of 3.5D covers the area around the pile that is susceptible to sediment mobility (1D from the pile edge) and an additional placement accuracy space of 0.5D. The side slopes were chosen with 45° for both layers. The maximum rock armour width of 4.5D was chosen as a representative value found in the field (Table 2). A width shift of 1D between the armour layer and the filter layer was considered for convenience. Regarding the scour protection height, a filter layer height of 0.4 m to account for placement accuracy was taken as a minimum. A maximum filter layer height of 0.6 m was adopted.

Parametric study of post- and pre-installed scour protection systems.

ID	Parameter	Parameter Scour		Width	Height
(000)	undisturbed flat s	eabed			
(1s1)	smaller S	0.5D	_	-	-
(1f1)	smaller S	0.5D	rock fill CP 45-180		
(1s2)	larger S	1.0D	_	_	_
(1f2)	larger S	1.0D	rock fill CP 45-180		
(200)	standard		filter CP45–125	5.0D	0.50 m
			armour LMA5-40	4.0D	0.77 m (3.25D ₅₀)
(2w1)	shorter width		filter CP45-125	4.5D	0.50 m
			armour LMA5-40	3.5D	0.77 m (3.25D ₅₀)
(2w2)	larger width		filter CP45-125	5.5D	0.50 m
			armour LMA5-40	4.5D	0.77 m (3.25D ₅₀)
(2h1)	smaller height		filter CP45-125	5.0D	0.40 m
			armour LMA5-40	4.0D	0.59 m (2.50D ₅₀)
(2h2)	larger height		filter CP45-125	5.0D	0.60 m
			armour LMA5-40	4.0D	0.95 m (4.00D ₅₀)
(2m1)	heavier armour		filter CP45-125	5.0D	0.50 m
			armour LMA40-200	4.0D	1.44 m (3.25D ₅₀)
(2d1)	dense+ armour		filter CP45-125	5.0D	0.50 m
			armour LMA5-40 d+	4.0D	0.77 m (3.25D ₅₀)
(2d2)	dense++ armour		filter CP45-125	5.0D	0.50 m
			armour LMA5-40 d++	4.0D	0.77 m (3.25D ₅₀)

Table 8 Resultant loads H_i and M_i at mudline level for different DLc based on the 5 MW NREL wind turbine (load data from Menéndez-Vicente et al., 2023).

DLc	(I)	(II)	(III)	(IV)
Wind	NTM at U_R	ETM at U_R	EOG at U_R	EOG at Uout
Wave	1-yr ESS	50-yr EWH	1-yr EWH	50-yr EWH
H [MN]	3.4	7.1	6.4	6.6
M [MNm]	167	302	354	242

The height of the armour layer was defined based on the median sieve size D_{50} . A minimum of $2.5D_{50}$ and a maximum of $4.0D_{50}$ were considered following design recommendations and references from the field (Table 2).

2.4. Loads

LU ratios were calculated based on standardised Design Load cases (DLc) used in previous studies (e.g. Bhattacharya, 2019; Aleem et al., 2022; Menéndez-Vicente et al., 2023). These DLc cover different wind and wave loading scenarios, from (I) normal operation to (II) extreme wave, and (III, IV) extreme wind loading. These DLc were calculated for the benchmark 5 MW wind turbine from the National Renewable Energy Laboratory (NREL) in Jonkman et al. (2009), and the metocean data found in Arany et al. (2017). Table 8 shows the wind and wave conditions for each DLc and the lateral force H and moment M loading. For the wind models, NTM (Normal Turbulence Model), ETM (Extreme Turbulence Model), and EOG (Extreme Operating Gust) were considered with the rated wind speed U_R and the cut-out wind speed U_{out} . For the wave models, ESS (Extreme Sea State), and EWH (Extreme Wave Height) were considered with 1 year or 50 years return periods. Readers are referred to Menéndez-Vicente et al. (2023) for further information on DLc. The LU ratios of the M-H curves of the large-diameter monopile model were calculated using these loads.

2.5. Validation

To validate the numerical results, the experimental data obtained through centrifuge modelling (100 g) and numerical data of the monotonic load tests performed by Askarinejad et al. (2022) were used. The small-diameter model described previously yielded the results presented in Figs. 3 and 4. In this case, the horizontal load was applied at the top of the structure as explained in their experimental analysis

to reproduce the model used for validation and allow comparability. It should be noted that, in analogy to the model in Askarinejad et al. (2022), the scour protection is simulated via a vertical pressure of 15 kPa around the pile. The curves in Fig. 4 show hence the force–displacement behaviour for a monopile with a scour protection equivalent pressure. For small displacements, both load–displacement curves agree, whereas for larger displacements a small overestimation of the load–displacement response is observed. In general, it is concluded that the previously described modelling strategy (Section 2.2) is valid and thus applied for further analysis of the soil–pile system. Moreover, as stated previously, it is noted that a rough interface (as also used in Askarinejad et al., 2022) yields a better estimation of the force–displacement response compared to the frictional law.

3. Results and discussion

3.1. M-H capacity

Small-diameter monopile.

The M-H curves obtained for the post-installed scour protection systems are presented in Fig. 5, where the curve (000) refers to the undisturbed flat case, (1s1) to the scoured monopile with S = 0.5D, (1f1) to its protection with rock fill, (1s2) to the scoured monopile with S = 1.0D, and (1f2) to its protection with rock fill. The M -H curves above the reference case (000) indicate a stiffer soil-pile system, whereas the curves below the reference indicate a softer system response. In the case of scour (1s1 and 1s2), the M-H capacity is considerably reduced due to the loss in embedment length and overburden pressure. It can be seen that for the larger scour depth (1s2, i.e. S = 1.0 D), only 0.8 of the original resisting moment and lateral force are carried by the foundation. This evidences the risk of scour on OWT and the need for scour protection mechanisms. Further investigation into the effects of scour on M-H capacity curves may be found in Menéndez-Vicente et al. (2023). For the scoured monopiles retrofitted with rock fill (1f1 and 1f2), the rock fill material provides sufficient stiffness to outperform the reference flat bed case (000), reaching higher capacities of approximately 5% (for S = 0.5D) and 10% (for S = 1.0D).

Figs. 6 and 7 analyse the effect of pre-installed scour protection for the cases with a smaller and larger width (2w1 and 2w2), with a smaller and larger height (2h1 and 2h2), with a heavier rock armour (2m1), and with a densified rock armour matrix (2d1 and 2d2) as defined

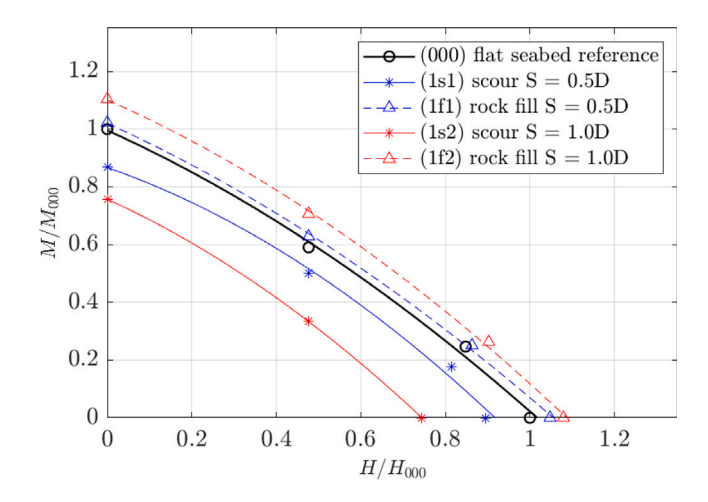


Fig. 5. M-H curves (small-diameter monopile) for scour depths and corresponding rock fill.

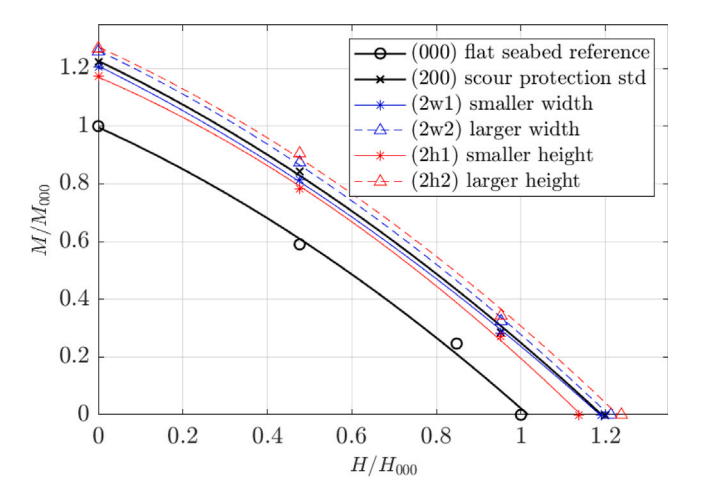


Fig. 6. M-H curves (small-diameter monopile) for different scour protection dimensions

in Table 7. The case (200) shows a standard scour protection system, which for the small-diameter monopile achieves increases in the M – H capacity of approximately 20%. For these monopile dimensions, implementing a scour protection mechanism achieves a significant improvement in terms of additional stiffness to the soil-pile system. The influence of the geometric parameters in terms of width (smaller width 2w1 and larger width 2w2) and height (smaller height 2h1 and larger height 2h2) is shown in Fig. 6. The main driver of increased stiffness is seen to be the increase in the height of the scour protection, rather than the expansion of the protection width. An increase in the scour protection height implies a larger overall embedded depth (i.e. the original embedment length plus the scour protection height). This produces a higher overburden pressure, which provides additional stiffness to the soil-pile system. However, the changes in the scour protection width only provide certain additional overburden pressure on the periphery of the scour protection system. Its effect on M-Hcapacity is therefore very limited and less significant compared to changes in the scour protection height.

The rock armour material properties are analysed in Fig. 7, where a heavier rock armour (2m1) with LMA40–200 instead of LMA5–40, used for the reference case (200), is implemented. The LMA 40–200 rock armour indirectly increases the scour protection height to fulfil the chosen height of $3.25D_{50}$. This armour height was chosen to be consistent with the reference case (200), as seen in Table 7. As explained

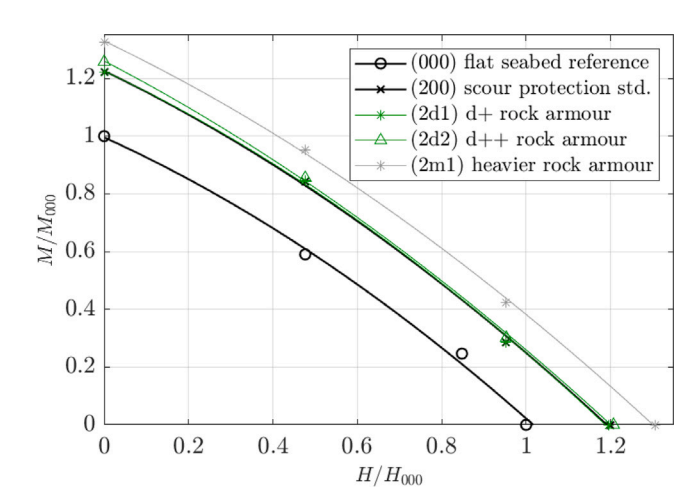


Fig. 7. M-H curves (small-diameter monopile) for different scour protection material properties.

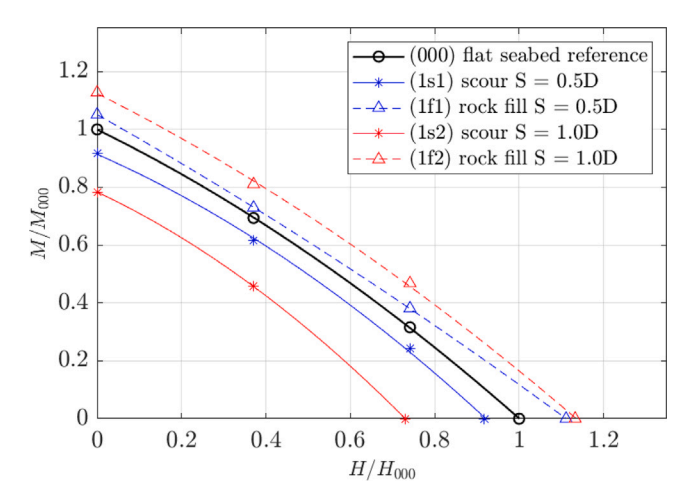


Fig. 8. M-H curves (large-diameter monopile) for scour depths and corresponding rock fill.

previously, common rock armour heights range between $2.5D_{50}$ and $4.0D_{50}$ as a stability criterion. This combination of a heavier material with a greater scour depth causes M-H increases of up to 30% for the small-diameter monopile being studied. Moreover, the effect of a potential densification of the armour through sand accretion is studied in cases (2d1) and (2d2). It can be observed that the changes in terms of M-H capacity for a potential densification through sand accretion are negligible.

Large-diameter monopile.

The M-H curves obtained for the large-diameter monopile are shown in Figs. 8 to 10. The post-installed rock fill (Fig. 8) yields a similar response in terms of M-H capacity compared to the small-diameter monopile. It is noted that the rock fill cases (1f1 and 1f2) achieve increases in M-H capacity of approximately 10% (for 1f1, i.e. rock fill of S=0.5D) and 20% (for 1f2, i.e. rock fill of S=1D), which are greater than those registered in the small-diameter case (Fig. 5).

For pre-installed scour protection systems, a similar qualitative behaviour of the M-H capacity is also observed for large-diameter monopiles. The height of the scour protection system has a greater influence in providing additional stiffness to the soil–pile system, whereas the width of the scour protection system does not induce a significant change in the foundation conditions (Fig. 9). Regarding the effect

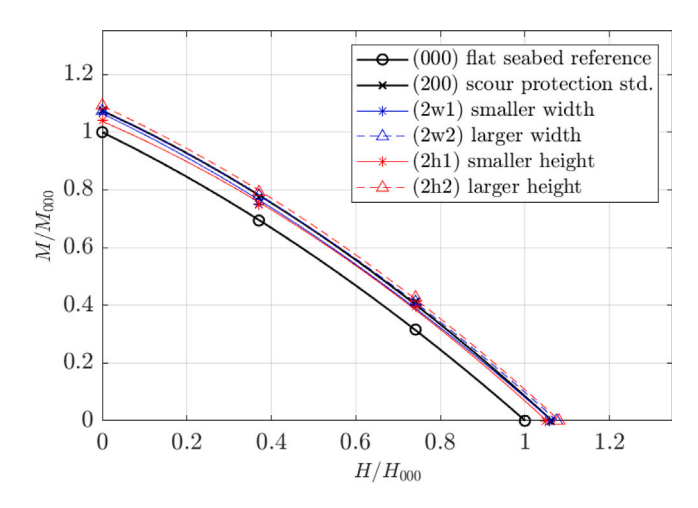


Fig. 9. M-H curves (large-diameter monopile) for different scour protection dimensions

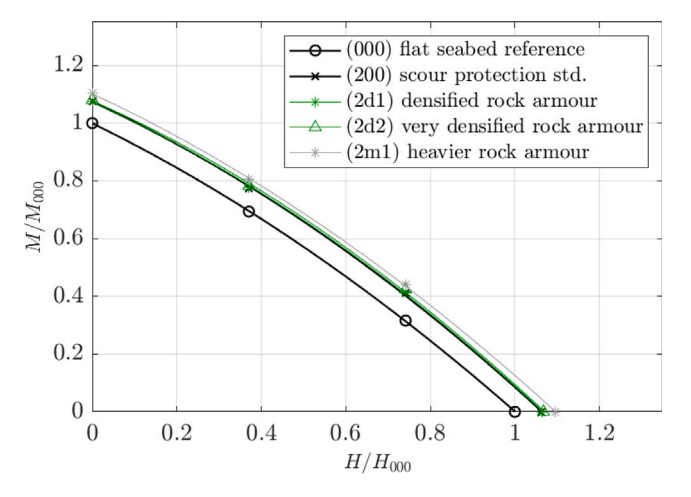


Fig. 10. M-H curves (large-diameter monopile) for different scour protection material properties.

of the material properties (Fig. 10), as previously observed, heavier rock armour (2m1) causes an increase in M-H capacity (approximately 4%), whereas the effect of the rock armour densification is practically negligible. Quantitatively, differences are evident between the small-diameter and the large-diameter monopiles for pre-installed scour protection systems. The reference scour protection system (200) of the large-diameter monopile achieves increases in M-H capacity of approximately 10% compared to 20% for the small-diameter case. Moreover, the differences between the geometrical and material parameters studied are considerably smaller. As an example, the difference observed between the reference case (200) and the geometrical cases (2w1, 2w2, 2h1, and 2h2) is less than 2% compared to 4% for the small-diameter analysis.

Discussion.

The presented results show that the scour protection systems considered in the present study provide stiffening to the foundation, leading to an increase in M-H capacity. For post-installed systems, the rock fill material contributes to a significant additional stiffness to the foundation, outperforming the case with the undisturbed flat bed. This conclusion differs from the experimental analysis in Mayall et al. (2020), in which they observed that post-installed systems did not achieve full restoration of the initial conditions. Different reasons may explain this divergence. Firstly, their study focused on the dynamic

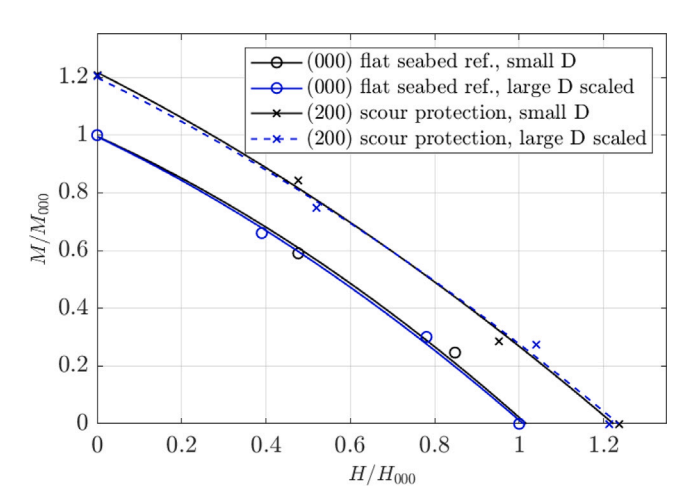


Fig. 11. M-H curves for the small-diameter monopile and the linearly scaled large-diameter monopile (ratio $H_P/L_p=0.141$ equal in both models).

performance rather than on the static capacity. As it is known, a pile subjected to a dynamic (cyclic) load may induce soil degradation, reducing its capacity to restore initial conditions even if rock fill material is placed. Secondly, in terms of FE analysis, the scour protection system is modelled as a solid body, which does not reproduce possible grain interactions between the rockfill–soil interface. Despite this, it is recommended to consider rock fill as a potential solution for already scoured monopiles for two reasons: to restore initial stiffness conditions and to prevent additional scouring. This conclusion is applicable to the small-diameter and the large-diameter monopiles, since a similar behaviour is observed in both cases. Further research of soil–pile dynamic performance or experimental modelling is needed to clarify whether full restoration of initial stiffness conditions is possible under real field conditions.

Pre-installed systems, however, are more effective in contributing to the foundation stiffness compared to post-installed systems, as also concluded in Mayall et al. (2020). For pre-installed systems, the diameter of the monopile has a significant influence on the effect that scour protection has on the foundation stiffness. Specifically, the dimensions of the monopile (diameter D and embedment length L_n) and the dimensions of the scour protection system are key parameters. The design scour protection height is not dependent on the pile dimensions, but on the material used (e.g. the rock armour is chosen between $2.50D_{50}$ and $4.0D_{50}$). Hence, for a large-diameter monopile, the stiffening effect of the scour protection is very limited, as seen in Fig. 9. The ratio of scour protection height to pile embedment length H_P/L_p is introduced. To ensure comparability between results and isolate the H_P/L_p ratio, additional simulations were carried out. The large-diameter monopile model with scour protection (200) was linearly scaled up with the diameter of the pile. Therefore, the ratio $H_P/L_p = 0.141$ found in the small-diameter case was also applied to the large-diameter monopile (i.e. the scour protection height increased to 5.29 m). Keeping the H_P/L_p ratio the same for both systems (small D and large D) allows comparability of the changes in the M-H capacity caused by scour protection systems. Fig. 11 shows the results of the flat bed case (000) and the reference pre-installed scour protection case (200) for both systems: the small-diameter and the large-diameter monopile (incl. linear scaling of the scour protection system with *D*). It is clearly seen that the curves yield very similar results, suggesting that the differences observed previously (between small-diameter and large-diameter monopiles) are due to the different H_P/L_p ratios.

This demonstrates that for small-diameter monopiles, pre-installed scour protection systems have a double purpose: increasing the foundation stiffness and preventing scour. For small-diameter monopiles, scour

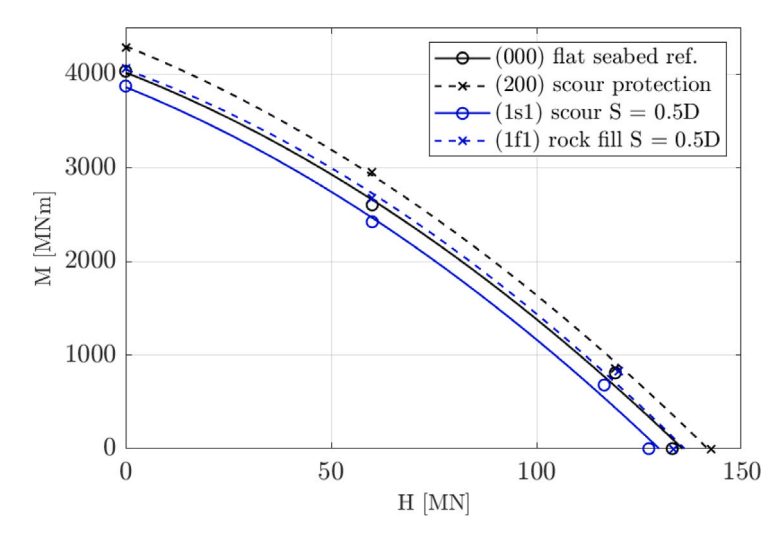


Fig. 12. M-H curve of the 5 MW NREL turbine supported by a large-diameter (D=7.5 m) monopile for selected cases: (000), (1s1), (1f1), and (200).

Table 9 LU ratios for DLc (I) to (IV) of the 5 MW NREL turbine supported by a large-diameter (D = 7.5 m) monopile.

Case	DLc (I)	DLc (II)	DLc (III)	DLc (IV)
(000) flat bed	16.6	8.6	8.2	10.2
(200) std. pre-installed scour protection	17.6	9.2	8.6	10.7
(1s1) scour S = 1.0 D	15.8	8.3	7.8	9.7
(1f1) rock fill of $S = 1.0 D$	16.8	8.8	8.3	10.3

protection thus needs to be considered to optimise foundation design. However, for large-diameter monopiles, pre-installed scour protection systems only achieve minor stiffening of the foundation. It is thus concluded that pre-installed scour protection is important to prevent scour, but it has a marginal role in providing additional foundation stiffness. However, it is still recommended to consider scour protection during foundation design and, more specifically, to plan foundations with heavier rock armour (e.g. LMA40–200) and heights of e.g. $\geq 4D_{50}$.

Regarding the parametric study of dimensions and rock armour properties, it is concluded that the scour protection width has only a minor effect, whereas the scour protection height is the key parameter that can induce changes in the foundation stiffness, as also suggested in Ma and Chen (2021). It is concluded that densification through sand accretion (or even marine growth), which is suggested in Mayall et al. (2020), is practically negligible in terms of additional stiffness. However, the use of a heavier material provides significant additional stiffness and is thus recommended in design.

3.2. Design chart and LU ratios

The M-H methodology used previously was applied to a real scenario: a large-diameter monopile supporting the 5 MW NREL turbine (Jonkman et al., 2009). Therefore, representative M-H curves of (000) the flat undisturbed bed, (1s1) the scoured monopile with $S=0.5\mathrm{D}$, (1f1) its post-installed rock fill, and (200) the standard preinstalled scour protection were calculated for a real scenario. For these curves, submerged conditions were considered. Fig. 12 shows the M-H curves for the aforementioned cases. Table 9 shows the LU ratios for the DLc explained previously. These curves and LU ratios are representative cases and serve as a design example for large-diameter monopiles. It has to be noted that moments M and lateral loads H are given at mudline level.

3.3. Natural frequencies

Monopile foundations are also liable to changes in their natural frequencies when scoured or protected against scour. FE analysis of the eigenmodes influenced by the scour protection parameters shown in Table 7 were conducted. Therefore, the large-diameter monopile with the 5 MW NREL turbine (Jonkman et al., 2009) was modelled. The eigenfrequencies for the reference flat bed case (000) are 0.2163 Hz in the fore-aft direction and 0.2167 Hz in the sideward direction. To validate these eigenfrequencies, the analytical method explained in Arany et al. (2017) was used, obtaining a natural frequency of 0.2198 Hz. The analytical method uses Eqs. (6) and (7), which are formulated based on the cantilever beam formula (f_{FB} is the tower natural frequency) modified with the coefficients C_L , C_R , and C_S . These coefficients account for the lateral foundation, rotational foundation, and substructure flexibilities respectively. The fixed base tower natural frequency is calculated as shown in Eq. (7), in which k_0 and m_0 are the equivalent stiffness and mass, respectively. Readers are referred to the publication of Arany et al. (2017) for further details. This analytical approach yields a very similar result to that obtained with FE analysis. Hence, the FE model was considered validated and used in the framework of the parametric study. Submerged conditions were considered to simulate the real offshore environment.

$$f_0 = C_L C_R C_S f_{FB} \tag{6}$$

$$f_{FB} = \frac{1}{2\pi} \sqrt{\frac{k_0}{m_0}} \tag{7}$$

The eigenmodes in the fore–aft direction and in the sideward direction are shown in Fig. 13, whereas the changes in natural frequencies are shown in Figs. 14 and 15. Table 10 shows the absolute values of the natural frequencies in [Hz] and the variation compared to the undisturbed flat seabed case (000). It is noted that scour causes significant reductions in the natural frequencies from 1% (for S=0.5D) to 2.5% (for S=1.0D). Post-installed scour protection achieves the stiffening of the foundation, outperforming the flat undisturbed seabed model. Regarding the pre-installed scour protection systems, variations in the scour protection width barely affect the natural frequencies, whereas variations in the height cause slight changes of up to 0.9%. A heavier rock armour (2m1) increases the natural frequencies (1%), whereas a densification of the matrix only produces very small increments of the natural frequencies.

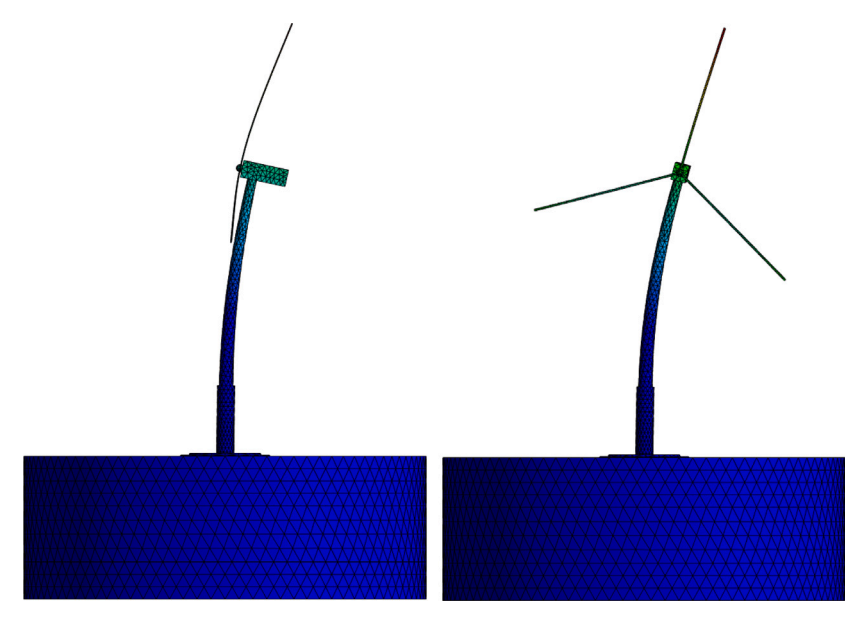


Fig. 13. First eigenmodes (l) in the fore-aft direction and (r) in the sideward direction.

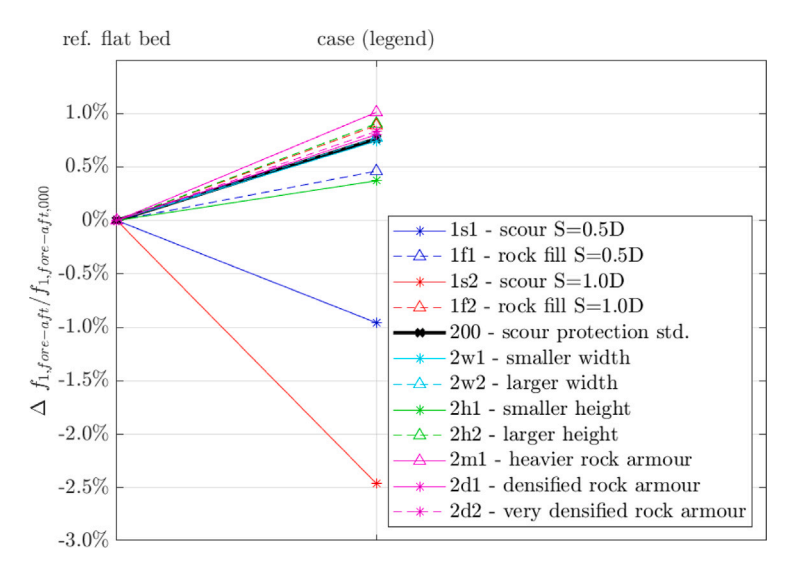


Fig. 14. Variations of the natural frequency in the fore-aft direction.

Discussion.

The results are comparable to those obtained for the static M-Hcapacity. It is seen that post-installed scour protections are effective in restoring initial conditions and should be used on the field if scourinduced changes in the natural frequencies are observed. Scour poses a significant risk to OWT, as the reduction of the natural frequency may force the structure to its loading frequencies, generating fatigue load cycles. Regarding pre-installed scour protection systems, it is seen that the construction of riprap around the monopile provides an additional stiffness and a shift of the natural frequency of approximately 0.8% away from the forcing frequencies. The parametric study of preinstalled protections shows that the heavier rock armour provides the highest stiffness to the foundation system. The differences between the shorter or the larger widths are negligible, whereas the scour protection height has only a small effect on the stiffness. Densification through sand accretion has only a marginal effect and is hence negligible. It may be concluded that pre-installed scour protection is more effective than post-installed systems and should thus be considered from early design stages. The differences between the eigenfrequencies in the fore-aft direction (Fig. 14) and in the sideward direction (Fig. 15) are negligible.

4. Conclusions

A parametric study of post-installed and pre-installed scour protection systems using M-H curves and natural frequencies was conducted to assess the impact of scour protection (its dimensions and material properties) on the foundation of monopiles supporting OWT. Through a series of FE analysis, the potential contribution of scour protection systems to the stiffness of the foundation has been investigated. The results and the discussion have yielded the following conclusions:

- Numerical analysis indicates that rock fill on a developed scour hole restores (and even increases) the initial foundation stiffness under static loading. Hence, a post-installed scour protection system is recommended as a potential solution to increase the weakened foundation stiffness and to prevent further scouring.
- A pre-installed scour protection system should be considered from early design stages and should be preferred over post-installed systems to prevent scour, avoid a shift of the natural frequency towards the forcing frequencies, and as a stiffness contributor (especially for small-diameter monopiles).

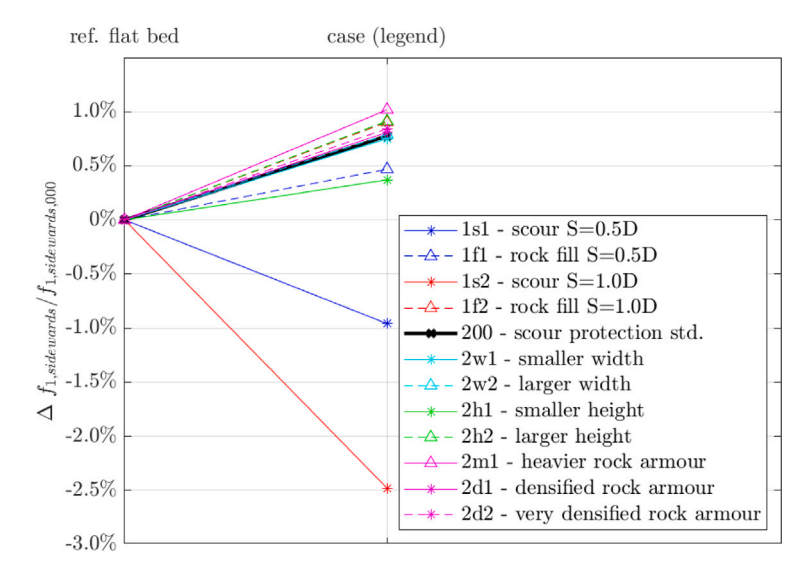


Fig. 15. Variations of the natural frequency in the sideward direction.

Table 10
Natural frequencies obtained with FE analysis.

Case		Fore–aft dire	ction	Sideward dire	Sideward direction		
(000)	undisturbed flat seabed	0.2163 Hz		0.2167 Hz			
(1s1)	scour $S = 0.5D$	0.2142 Hz	-1.0%	0.2147 Hz	-0.9%		
(1f1)	rock fill of $S = 0.5D$	0.2172 Hz	+0.4%	0.2177 Hz	+0.5%		
(1s2)	scour $S = 1.0D$	0.2109 Hz	-2.5%	0.2113 Hz	-2.5%		
(1f2)	rock fill of $S = 1.0D$	0.2181 Hz	+0.9%	0.2187 Hz	+0.9%		
(200)	std. pre-installed scour protection	0.2179 Hz	+0.7%	0.2185 Hz	+0.8%		
(2w1)	shorter width	0.2179 Hz	+0.7%	0.2184 Hz	+0.8%		
(2w2)	larger width	0.2180 Hz	+0.8%	0.2185 Hz	+0.8%		
(2h1)	smaller height	0.2170 Hz	+0.3%	0.2175 Hz	+0.4%		
(2h2)	larger height	0.2182 Hz	+0.9%	0.2187 Hz	+0.9%		
(2m1)	heavier armour	0.2184 Hz	+1.0%	0.2189 Hz	+1.0%		
(2d1)	dense+ armour	0.2180 Hz	+0.8%	0.2185 Hz	+0.8%		
(2d2)	dense++ armour	0.2181 Hz	+0.8%	0.2185 Hz	+0.9%		

- The analysis shows that the scour protection height to pile embedment length ratio H_P/L_p has a significant influence in determining how scour protection affects the foundation stiffness. For small-diameter monopiles (with shorter embedment lengths and larger H_P/L_p ratios), it is recommended to consider the stiffness contribution of scour protection to optimise foundation design. For these small-diameter monopiles, scour protection fulfils the purpose of preventing scour and providing additional stiffness.
- For large-diameter monopiles (with longer embedment lengths and smaller H_P/L_p ratios), scour protection may be considered as a foundation stiffness contributor for heavy materials and thick rock armour layers. The numerical analyses have shown that the static capacity is increased by 10% in these cases. However, the main benefit of scour protection systems around large-diameter monopiles is preventing scour.
- As may be expected, pre-installed scour protection increases the *M-H* capacity of monopiles. However, from this study it is found that the height of the scour protection is the key parameter that provides additional stiffness to the soil–pile system of approximately +8%. Nonetheless, it is noted that a higher rock armour may cause edge scour of the scour protection system. The width of the scour protection is of secondary relevance.
- The use of a heavier rock armour material (e.g. LMA40–200 instead of LMA5–40) significantly increases the static M H capacity for small-diameter and large-diameter monopiles by approximately 10%. It is hence recommended that these types of scour protection systems are put forward for foundations highly exposed to scour and significant environmental loading.

- This study proves that a potential densification of the armour matrix through sand accretion or marine growth does not significantly affect the M-H capacity of the system (less than 1%) and it may be neglected in foundation design.
- Scour and scour protection performance require close monitoring in the field and consequent evaluation with accurate numerical modelling. The present parametric study indicates that variations in the dimensions and properties of scour protection may influence the M-H capacity and the natural frequencies considerably. To assess how this affects the static capacity, the present methodology (M-H curves and Load Utilisation ratios) has proven to be an effective tool.

These conclusions may also be applicable to other types of piled foundations exposed to lateral and moment loading, such as jackets, tripods or bridge piers. From this study it is concluded that scour needs to be addressed as a geological hazard and that scour protection systems should be implemented to reduce uncertainties in a changing geological marine environment.

Funding

This work was supported by the BritishSpanish Society scholarship (Plastic Energy, 2023) obtained by Carlos Menéndez-Vicente.

CRediT authorship contribution statement

Carlos Menéndez-Vicente: Writing – review & editing, Writing – original draft, Visualization, Validation, Methodology, Investigation,

Formal analysis, Conceptualization. **Susana López-Querol:** Writing – review & editing, Supervision, Methodology, Conceptualization. **John M. Harris:** Writing – review & editing, Conceptualization. **Nicholas S. Tavouktsoglou:** Writing – review & editing, Conceptualization.

Declaration of competing interest

The authors declare the following financial interests/personal relationships which may be considered as potential competing interests: Carlos Menendez-Vicente reports financial support was provided by BritishSpanish Society (scholarship 2023 by Plastic Energy). If there are other authors, they declare that they have no known competing financial interests or personal relationships that could have appeared to influence the work reported in this paper.

Acknowledgements

We would like to gratefully acknowledge the expertise provided by Prof. Richard Simons from University College London, United Kingdom. We would also like to thank the BritishSpanish Society and Plastic Energy for their support.

Data availability

Data will be made available on request.

References

- Achmus, M., Kuo, Y.S., Abdel-Rahman, K., 2009. Behavior of monopile foundations under cyclic lateral load. Comput. Geotech. 36 (5), 725–735. http://dx.doi.org/10. 1016/j.compgeo.2008.12.003.
- Aleem, M., Bhattacharya, S., Cui, L., Amani, S., Salem, A., Jalbi, S., 2022. Load utilisation (LU) ratio of monopiles supporting offshore wind turbines: Formulation and examples from European wind farms. Ocean Eng. 248, http://dx.doi.org/10. 1016/j.oceaneng.2022.110798.
- Arany, L., Bhattacharya, S., Macdonald, J., Hogan, S., 2017. Design of monopiles for offshore wind turbines in 10 steps. Soil Dyn. Earthq. Eng. 92, 126–152. http://dx.doi.org/10.1016/j.soildyn.2016.09.024.
- Askarinejad, A., Wang, H., Chortis, G., Gavin, K., 2022. Influence of scour protection layers on the lateral response of monopile in dense sand. Ocean Eng. 244, 110377. http://dx.doi.org/10.1016/j.oceaneng.2021.110377.
- Azúa-González, C.X., Zeben, J., Alvarez Grima, M., Hof, C., Askarinejad, A., 2019. Dynamic FE analysis of Soft Boundary (SB) effects on impact pile driving response in centrifuge tests. In: XVII European Conference on Soil Mechanics and Geotechnical Engineering in Reykjavik. Iceland, http://dx.doi.org/10.32075/17ECSMGE-2019-0821
- Bhattacharya, S., 2019. Design of Foundations for Offshore Wind Turbines. Wiley, http://dx.doi.org/10.1002/9781119128137.
- Chortis, G., 2018. Numerical Investigation on the Effect of Scour Formation & Scour Protection on the Stiffness & Lateral Capacity of Monopiles. Delft University of Technology.
- CIRIA/CUR/CETMEF, 2007. The Rock Manual: The Use of Rock in Hydraulic Engineering, second ed. (C683).
- Cuéllar, P., 2011. Pile foundations for offshore wind turbines: Numerical and experimental investigations on the behaviour under short-term and long-term cyclic loading. http://dx.doi.org/10.14279/depositonce-2760.
- De Vos, L., De Rouck, J., Troch, P., Frigaard, P., 2011. Empirical design of scour protections around monopile foundations: Part 1: Static approach. Coast. Eng. 58 (6), 540–553. http://dx.doi.org/10.1016/j.coastaleng.2011.02.001.
- De Vos, L., De Rouck, J., Troch, P., Frigaard, P., 2012. Empirical design of scour protections around monopile foundations. Part 2: Dynamic approach. Coast. Eng. 60, 286–298. http://dx.doi.org/10.1016/j.coastaleng.2011.11.001.
- Esteban, M.D., López-Gutiérrez, J.S., Negro, V., Sanz, L., 2019. Riprap Scour Protection for Monopiles in Offshore Wind Farms. J. Mar. Sci. Eng. 7 (12), 440. http://dx.doi.org/10.3390/jmse7120440.
- Fazeres-Ferradosa, T., Chambel, J., Taveira-Pinto, F., Rosa-Santos, P., Taveira-Pinto, F.V.C., Giannini, G., Haerens, P., 2021. Scour Protections for Offshore Foundations of Marine Energy Harvesting Technologies: A Review. J. Mar. Sci. Eng. 9 (3), http://dx.doi.org/10.3390/jmse9030297.
- G+ Offshore Wind, 2017. WTG Decommissioning Project Robin Rigg Offshore Wind Farm. Case study. G+ Global Offshore Wind Health and Safety Organisation, https://www.gplusoffshorewind.com/?a=420541.

- Hampton, M.A., Lee, H.J., Locat, J., 1996. Submarine landslides. Rev. Geophys. 34 (1), 33–59. http://dx.doi.org/10.1029/95RG03287.
- Hansen, E., Nielsen, A., Høgedal, M., Simonsen, H., 2007. Scour Protection around Offshore Wind Turbine Foundations, Full-Scale Measurements. In: Scientific Proceedings of the European Wind Energy Conference 2007. EWEC 2007.
- Harris, J., Whitehouse, R., Tavouktsoglou, N., Godinho, P., 2019. Foundation scour as a geohazard. J. Waterw. Port Coast. Ocean Eng. 6, http://dx.doi.org/10.1061/(ASCE) WW.1943-5460.0000523.
- Hough, B., 1957. Basic Soils Engineering. Ronald Press, New York.
- Hsu, Y.H., Lu, Y.C., Khoshnevisan, S., Juang, H., Hwang, J.h., 2022. Influence of geological uncertainty on the design of OWTF monopiles. Eng. Geol. 303, 106621. http://dx.doi.org/10.1016/j.enggeo.2022.106621.
- Jonkman, J., Butterfield, S., Musial, W., Scott, G., 2009. Definition of a 5-MW Reference Wind Turbine for Offshore System Development. National Renewable Energy Laboratory (NREL), Golden, Colorado, USA, http://dx.doi.org/10.2172/947422.
- Le, T.M.H., Eiksund, G.R., Strøm, P.J., Saue, M., 2014. Geological and geotechnical characterisation for offshore wind turbine foundations: A case study of the sheringham shoal wind farm. Eng. Geol. 177, 40–53. http://dx.doi.org/10.1016/ j.enggeo.2014.05.005.
- LeBlanc, C., Houlsby, G., Byrne, B., 2010. Response of stiff piles in sand to long-term cyclic lateral loading. Géotechnique 60 (2), 79–90. http://dx.doi.org/10.1680/geot. 7.00196
- Lopez-Querol, S., Spyridis, M., Moreta, P.J.M., Arias-Trujillo, J., 2020. Simplified Numerical Models to Simulate Hollow Monopile Wind Turbine Foundations. J. Mar. Sci. Eng. 8 (11), http://dx.doi.org/10.3390/jmse8110837.
- Louwersheimer, W., Verhagen, H., Olthof, J., 2009. Scour around an offshore wind turbine. Coast. Struct. 1903-1912 http://dx.doi.org/10.1142/9789814282024_0168.
- Ma, H., Chen, C., 2021. Scour protection assessment of monopile foundation design for offshore wind turbines. Ocean Eng. 231, 109083. http://dx.doi.org/10.1016/j. oceaneng.2021.109083.
- Matutano, C., Negro, V., López-Gutiérrez, J.S., Esteban, M.D., Hernández, A., 2014.
 The effect of scour protections in offshore wind farms. J. Coast. Res. 70, 12–17.
 http://dx.doi.org/10.2112/SI70-003.1.
- Mayall, R., 2019. Monopile Response to Scour and Scour Protection (Ph.D. thesis). University of Oxford.
- Mayall, R.O., McAdam, R.A., Whitehouse, R.J.S., Burd, H.J., Byrne, B.W., Heald, S.G., Sheil, B.B., Slater, P.L., 2020. Flume Tank Testing of Offshore Wind Turbine Dynamics with Foundation Scour and Scour Protection. J. Waterw. Port Coast. Ocean Eng. 146 (5), 04020033. http://dx.doi.org/10.1061/(ASCE)WW.1943-5460. 0000587.
- Menéndez-Vicente, C., López-Querol, S., Bhattacharya, S., Simons, R., 2023. Numerical study on the effects of scour on monopile foundations for Offshore Wind Turbines: The case of Robin Rigg wind farm. Soil Dyn. Earthq. Eng. 167, 107803. http://dx.doi.org/10.1016/j.soildyn.2023.107803.
- Nielsen, A.W., Liu, X., Sumer, B.M., Fredsøe, J., 2013. Flow and bed shear stresses in scour protections around a pile in a current. Coast. Eng. 72, 20–38. http: //dx.doi.org/10.1016/j.coastaleng.2012.09.001.
- Pan, K., Yuan, Z., Zhao, C., Tong, J., Yang, Z., 2022. Undrained shear and stiffness degradation of intact marine clay under monotonic and cyclic loading. Eng. Geol. 297, 106502. http://dx.doi.org/10.1016/j.enggeo.2021.106502.
- Raaijkmakers, T., 2009. Evaluation of performance of scour protection and edge scour development: Egmond aan Zee. Deltares.
- Saathoff, J.E., Goldau, N., Achmus, M., Schendel, A., Welzel, M., Schlurmann, T., 2024. Influence of scour and scour protection on the stiffness of monopile foundations in sand. Appl. Ocean Res. 144, 103920. http://dx.doi.org/10.1016/j.apor.2024. 103920.
- Sarmiento, J., Guanche, R., Iturrioz, A., Ojanguren, T., Ávila, A., Yanes, C., 2021.
 Experimental Evaluation of Dynamic Rock Scour Protection in Morphodynamic Environments for Offshore Wind Jackets. Energies 14(12), 3379, http://dx.doi.org/10.3390/en14123379.
- Tavouktsoglou, N.S., 2018. Scour and Scour Protection Around Offshore Gravity Based Foundations (Doctoral thesis) (Eng.D). University College London.
- Whitehouse, R.J.S., Brown, A.M., Audenaert, S., Bolle, A., de Schoesitter, P., Haerens, P., Baelus, L., Troch, P.A., das Neves, L., Ferradosa, T., Pinto, P., 2014. Optimising scour protection stability at offshore foundations. In: 7th International Conference on Scour and Erosion. ICSE in Perth, Australia.
- Whitehouse, R.J., Harris, J.M., Sutherland, J., Rees, J., 2011. The nature of scour development and scour protection at offshore windfarm foundations. Marine Poll. Bull. 62 (1), 73–88. http://dx.doi.org/10.1016/j.marpolbul.2010.09.007.
- Xu, D., Abadie, C., Madabhushi, G., Harris, J., Whitehouse, R., 2022. Response of armour rock-scour protection to earthquake-induced liquefaction for offshore wind applications. In: 10th International Conference on Physical Modelling in Geotechnics. ICPMG in Daejon, Korea.
- Zhou, Y.G., Chen, J., Chen, Y.M., Kutter, B.L., Zheng, B.L., Wilson, D.W., Stringer, M.E., Clukey, E.C., 2017. Centrifuge modeling and numerical analysis on seismic site response of deep offshore clay deposits. Eng. Geol. 227, 54–68. http://dx.doi.org/ 10.1016/j.enggeo.2017.01.008, New Advances in Coastal Engineering Geology and Geotechnics.
- Zhu, C., Peng, J., Jia, Y., 2023. Marine geohazards: Past, present, and future. Eng. Geol. 323, 107230. http://dx.doi.org/10.1016/j.enggeo.2023.107230.